12.Performance of Microtabs and Trailing Edge Flap

by I Satiawan

Submission date: 05-Jun-2023 07:44AM (UTC-0500)
Submission ID: 2109475636
File name: Trailing_Edge_Flaps_in_Wind_Turbine_Power_Regulation_AWTSim.pdf (561.01K)
Word count: 6961
Character count: 34242

JREE: Vol. 9, No. 2, (Spring 2022) 18-26

Journal of Renewable Energy and Environment

Journal Homepage: www.jree.ir

Materials and Energy Research Center

MERC

Research Article

Performance of Microtabs and Trailing Edge Flaps in Wind Turbine Power Regulation: A Numerical Analysis Using WTSim

Alireza Maheri[a*], I. Kade Wiratama[b], Terence Macquart[c]

[a] School of Engineering, Centre for Energy Transition, University of Aberdeen, Aberdeen, Scotland, United Kingdom.
[b] Faculty of Engineering, University of Mataram, Mataram, West Nusa Tenggara, Indonesia.
[c] Department of Aerospace Engineering, University of Bristol, Bristol, England, United Kingdom.

PAPER INFO

Paper history:
Received: 27 June 2021
Revised in revised form: 15 November 2021
Scientific Accepted: 10 September 2021
Published: 20 February 2022

Keywords:
Microtab,
Trailing Edge Flap,
Smart Blade,
Power Control,
Load Alleviation,
WTSim

ABSTRACT

The effectiveness of trailing-edge flaps and microtabs in damping 1P-3P loads has been proven through a series of research work during the past decade. This paper presents the results of an investigation into the effectiveness of these devices in power enhancement and power control for responding to the issue of where these devices can be used with dual function of load and power control on a medium size turbine. The 300 kW-AWT27 wind turbine is used as the base wind turbine and the effects of adding trailing-edge flaps and string of microtabs of different lengths positioned at different span locations on the aerodynamic performance of the rotor are studied. In each case, the wind turbine simulator WTSim is used to obtain the aerodynamic performance measures. In the next step, the original blade twist is redesigned to ensure that the blade is optimized upon the addition of these active flow controllers. It is found that blades equipped with flaps can increase the annual average power and reduce the blade loading at the same time for constant speed and variable speed generators. Power enhancement is more visible on constant speed rotors, while load reduction is more significant on variable speed rotors. To achieve constant speed rotors, an average power enhancement of around 12 % is achieved for a flap of size 25 % of the blade span located at about 72 % of the blade span. Microtabs are less effective in power control and can improve the produced power only by a few percentage points.

https://doi.org/10.30501/jree.2021.291397.1220

1. INTRODUCTION

Power and aerodynamic load control systems in wind turbines have multiple functions. All wind turbines need a power control system, which improves the extracted wind power at wind speeds below the rated wind speed and regulates the power at its rated value above the rated wind speed. In large-scale wind turbines, the blades experience significant loads. Hence, load alleviation becomes also a function of control systemin order to reduce the quasi-steady loads on blades due to gradual change in wind speed or in azimuth angle and/or to damp unsteady fluctuating loads, which are mainly produced by wind turbulence. Reducing fatigue loads produced by cyclic or stochastic forces due to tower shadow, yaw misalignment, wind shear, wind turbulence, and the wake effects of other turbines can result in a significant reduction in cost [1]. This remains a motivation for many research works during the past two decades, with growing interests in the past few years. These research works have focused on a variety of concepts for load reduction, some rooted in the already existing and well-established fixed-wing and rotary wing aircraft systems, and some specifically developed for wind turbines. A review of the state-of-the-art research in this field can be found in [1-3].

Conventional and some of the nonconventional power and load control mechanisms are shown in Figure 1. The control systems shown in this figure use different controlling parameters to control the power and/or load. Since the power extracted by a blade is in close relation to the aerodynamic load on the blade, some of these control systems inherently affect both power and load. The control parameters are blade span, aerofoil topology, and blade twist. Some of these control systems respond only to wind variations on large time scales, while some others have a shorter response time and can, therefore, be used for controlling the effect of wind variations with smaller timescales.

Controllers affecting the blade twist influence the performance of wind turbines by varying angles of attack α and the flow kinematics. As shown in Figure 1, the angle of attack depends on the inflow angle φ, elastic twist of the blade β_e, blade pretwist β_0, and pitch angle pitch. Collective and individual pitch control systems employ pitch as the controlling parameter. Bend-twist or stretch-twist adaptive

*Corresponding Author's Email: alireza.maheri@abdn.ac.uk (A. Maheri)
URL: https://www.jree.ir/article_145119.html

Please cite this article as: Maheri, A., Wiratama, I.K. and Macquart, T., "Performance of microtabs and trailing edge flaps in wind turbine power regulation: A numerical analysis using WTSim", *Journal of Renewable Energy and Environment (JREE)*, Vol. 9, No. 2, (2022), 18-26. (https://doi.org/10.30501/jree.2021.291397.1220).

blades control the performance by the blade elastic torsional displacement β_e which is produced as a result of elastic coupling in the blade material. Those controllers affecting the cross-sectional topology of the blade (e.g., via morphing or deploying an active flow controller) affect the form of the function $\vec{f}$ relating the aerodynamic coefficients C_L, C_D, and C_M to the flow kinematics.

Most of modern wind turbines use individual pitch control systems for alleviating loads of 1P (rotor rotational frequency) [4] up to 3P [5]. However, these systems do not have any significant impact on stochastic loads with higher frequencies. Furthermore, IPC exacerbates pitch actuations leading to an increase in wear and risk of failure of the blade-root connection. On the other hand, smaller active flow controllers, such as microtabs and trailing edge flaps, modify the flow kinematics locally instead of changing the flow kinematics around the entire of the blade [6, 7]. This led the researchers to investigating the potential benefits of implementation of these active flow controllers as auxiliary control surfaces for providing more effective load alleviation, particularly in damping fluctuating and stochastic loads with higher frequencies [8-13].

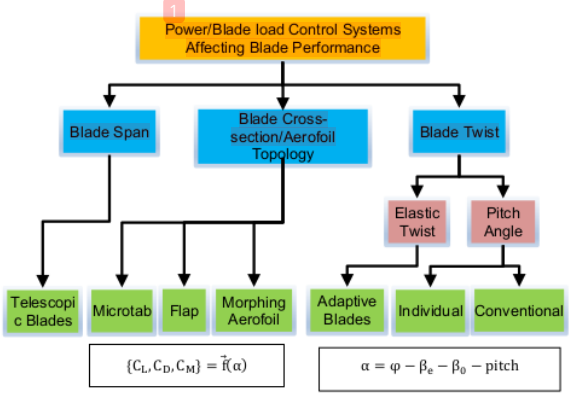

Figure 1. Different control systems affecting blade performance

Although the results of the above-mentioned studies have proven the potentials of these active flow controllers in load alleviation, utilization of these devices may take some time to be realized due to two main drawbacks of these systems. First, the integration of active flow controllers in wind turbine blades makes the blade manufacturing process more complicated due to required alteration in the process, particularly necessary modifications in moulding process and adding precise machining. Second, the integration of active flow controllers in wind turbine blades means the addition of moving mechanical parts to the structure of the blade. The maintenance and reliability of these systems become another concern for blade manufacturers.

Given that the previous research has focused on load alleviation and assumed that active flow controllers are accompanied by the main controller such as pitch system (for instance, see [14]) with the function of improving power at low winds and regulating the power at high winds, the capability of these devices in power control has not been investigated thoroughly. If these systems are capable of controlling the power as well as load alleviation, there will not be a need for the main control system and significant cost saving over the lifespan of the wind turbine can be achieved. This issue together with their proven potential in load alleviation and extension of the lifespan of the blades could circumvent the above-mentioned drawbacks. Ebrahimi and Movahhedi [15] conducted a numerical simulation of the performance of microtabs in improving the power of a 20-kW stall-regulated wind turbine below rated wind speed. Their results show some improvement in the average power for this small wind turbine. However, the issue of the suitability of microtabs for larger wind turbines remains unanswered.

In view of the above discussion, this paper aims to investigate the potential benefits of these control systems in power enhancement and regulation and to explore the possibility of using these devices as the only controlling systems with both functions of load alleviation and power regulation.

2. BLADES UTILIZING NONCONVENTIONAL CONTROL SURFACES

A wind turbine blade is defined by its span, chord, pretwist, aerofoil, and maximum thickness distributions: $\{R, c(r), \beta_0(r), AF(r), t_{max}(r)\}$. Three more parameters, namely inboard radial location $R_{F,s}$, outboard radial location $R_{F,e}$, and width of the flap as a fraction of the chord length at the centre of the flap $d_F^* = d_F/c_F$, are also required to define the location and size of the flap. These parameters are shown in Figure 2.

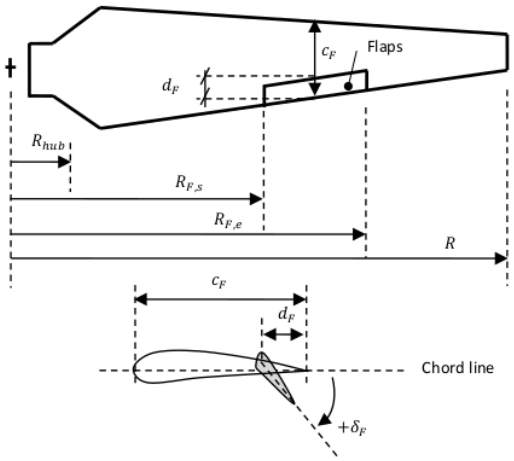

Figure 2. Blade with trailing edge flap

Once a flap is deployed by an angle of δ_F, it changes the flow kinematics around the blade at that location. This leads to a change in local lift and drag coefficients $\Delta C_L|_{\delta_F}$ and $\Delta C_D|_{\delta_F}$:

$$\Delta C_L|_{\delta_F} = C_L|_{\delta_F} - C_L|_{\delta_F=0} \quad (1.a)$$

$$\Delta C_D|_{\delta_F} = C_D|_{\delta_F} - C_D|_{\delta_F=0} \quad (1.b)$$

where, $C_L|_{\delta_F}$ and $C_D|_{\delta_F}$ are the aerodynamic coefficients at that deployment angle δ_F, and $C_L|_{\delta_F=0}$ and $C_D|_{\delta_F=0}$ are the original aerodynamic coefficients ($\delta_F = 0$). Besides the deployment angle, ΔC_L and ΔC_D depend on the aerofoil shape, flap width, and the angle of attack of the aerofoil α.

In case of blades equipped with microtabs, five parameters are required to define a string of microtabs on a blade. These parameters are the inboard and outboard radial locations of the string of microtabs $R_{MT,s}$ and $R_{MT,e}$; normalized distance from the leading edge $d^*_{MT} = d_{MT}/c_{MT}$; microtab length s_{MT} and actuation height $h^*_{MT} = h_{MT}/c_{MT}$. The distance from the leading edge and the actuation height are normalized by c_{MT}, which is the chord length at the centre of microtab. These parameters are shown in Figure 3.

Each microtab, in a string of microtabs, depending on its location can get two positions. Microtabs on the suction side of the aerofoil can be deployed upward only (coded by -1), while those on the pressure side of the aerofoil can be deployed downward (coded by +1). A deployed microtab changes lift and drag coefficients. These changes can be presented as follows:

$$\Delta C_L|_{MT} = C_L|_{MT} - C_L|_{MT=0};\ \ MT \in \{-1, +1\} \quad (2.a)$$

$$\Delta C_D|_{MT} = C_D|_{MT} - C_D|_{MT=0};\ \ MT \in \{-1, +1\} \quad (2.b)$$

where, $\Delta C_L|_{MT}$ and $\Delta C_D|_{MT}$ are the variations in aerodynamic coefficients as a result of the deployment of a microtab on the suction side ($MT = -1$) or pressure side ($MT = +1$); $C_L|_{MT}$ and $C_D|_{MT}$ are the aerodynamic coefficients; and $C_L|_{MT=0}$ and $C_D|_{MT=0}$ are the original aerodynamic coefficients without the presence or the deployment of microtabs. The amount of changes in lift and drag coefficients, ΔC_L and ΔC_D, depends on the local angle of attack, α, microtab location d^*_{MT}, and actuation height h^*_{MT}. An undeployed microtab in its neutral position has no effect on the flow kinematics.

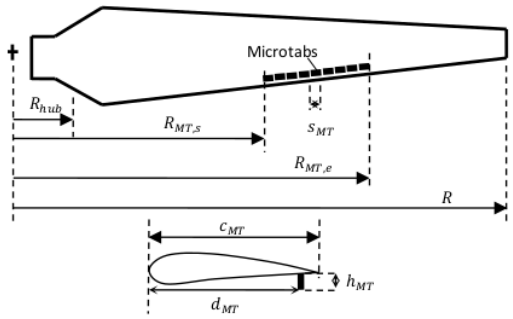

Figure 3. Blade with a string of microtabs

The analysis tool used for this study, WTSim (Wind Turbine Simulator), has a BEMT-based (blade element momentum theory) aerodynamic module and a controller simulator. This tool is capable of simulation of wind turbines with conventional and nonconventional blades (adaptive blades, telescopic blades, and blades equipped with active flow controllers). WTSim calculates the wind turbine aerodynamic performance, including the blade and rotor aerodynamic loads, blade internal forces, the rotor mechanical power in a given operating condition, and the annual average power. More information on the application of WTSim and the background theory of simulating smart blades can be found in [16] and [17], respectively. The BEMT module in WTSim is a modified version of that reported in [18] and [9]. The original version uses axial induction factor convergence algorithms [19 and 20] and is evaluated against WTPerf in [18] and against FAST and DU_SWAMP in [9] for conventional blades. This module has been modified for blades equipped with microtabs and trailing edge flaps.

For this study, the lookup tables for ΔC_L and ΔC_D due to the presence of mictotabs and flaps are obtained using XFOIL [21].

3. PRETWIST MODIFICATION

Since the addition of microtab or flap to the blade changes the flow kinematics around the blade, the original topology will not be optimum anymore. That is, we need to redesign the blade to ensure it is optimized for the new purpose. However, if we redesign the entire of the blade topology (chord, pretwist, and aerofoil distributions) and the rotor radius, we lose our ground for evaluating how much of the improvement results from the added active controller. Therefore, this study redesigns the pretwist distribution only. The pretwist has the highest effect on the flow kinematics around the blade; on the other hand, changing the pretwist does not directly lead to a change in the blade mass (as opposed to changing the chord and aerofoil distribution or rotor radius).

In all cases, the blade is modified to ensure that the full potential of active flow controllers is achieved without increasing the cost or the mass of the blade (except for the added cost or mass of the active flow controller itself). The optimization problem is, therefore, formulated as follows:

$$\max P_{av} = \int_{V_i}^{V_o} P(V)R(V)dV \quad (3.a)$$

subject to:

$$P \le P_{rated} \quad (3.b)$$

$$m_{blade,opt} \le m_{blade,original} \quad (3.c)$$

where P_{av} is the annual average power produced by the wind turbine if installed on a site with an average wind speed of V_{av}, $P(V)$ is the rotor power at wind speed V, $R(V)$ is the wind speed probability density function, V_i and V_o are the cut-in and cut-out velocities, respectively, P_{rated} is the rated power, and m_{blade} is the mass of the blade. Generally speaking, to ensure that Constraint (3.c) above is satisfied, we need to analyze the blade both aerodynamically and structurally. However, since the rotor radius and the chord and aerofoil distributions remain the same as the original blades, there is no need to increase the thickness of the blade shell and, hence, increase the mass of the blade if the loading on the optimized blade is equal to or less than the loading on the original blade. In other words, Constraint (3.c) is automatically satisfied if the following constraint on the flap bending moment, as the dominant load, is satisfied:

$$M_{flap,opt} \le M_{flap,original} \quad (3.d)$$

By replacing Constraint (3.c) with Constraint (3.d) and keeping the rotor radius, chord and aerofoil distributions constant, there is no need to include any structural analysis in the optimization process. This study calculates the average power based on a Rayleigh probability density function and site average wind speed of $V_{av} = 5.7\ m/s$ and cut-in and cut-out velocities of $V_i = 5\ m/s$ and $V_o = 25\ m/s$, respectively.

The optimization tool employed for solving this optimization problem is a Genetic Algorithm (GA) that

requires the BEMT module and the controller simulator for evaluating the design candidates (for calculating $P(V)$, $M_{flap}(V)$, and (P_{av}). The GA has special features such as geometric crossover for better exploitation of the solutions, dynamic mutation, and semi-heuristic initial population generation [22, 23]. A chromosome containing the aerodynamic design variables of a blade is a string of real numbers, integer numbers/coded parameters representing the chord, pretwist, and aerofoil distributions at some design points (n_{dp}) along the span of the blade. For blades equipped with mictotabs and flaps, assuming that the size and chordwise locations of these flow controllers are fixed, their span locations ($R_{F,s}, R_{F,e}, R_{MT,s}, R_{MT,e}$) are also added to the set of design variables.

4. POTENTIALS OF TRAILING EDGE FLAPS IN POWER ENHANCEMENT AND REGULATION

AWT27 wind turbine is adopted as the baseline turbine for this study. It is a two-bladed stall-regulated constant-speed wind turbine with a rotor diameter of 27.4 m. The blade profile is made of S800 series aerofoils. The rotor produces a rated power of about 300 kW at a rotor speed of 53.3 rpm. This turbine is a well-known research wind turbine with its technical data available in the public domain (e.g., see [24]). The advantage of AWT27 over newer research wind turbines such as variable-speed pitch-controlled NREL 5MW turbine is due to its type. A stall-regulated constant-speed turbine makes an ideal test case for studying the power control capabilities of control systems under investigation as it does not have any form of active control in place.

We deal with three design variables when conducting a design optimization of blades equipped with trailing edge flaps. These parameters are blade pretwist distribution, flap location, and flap length. As shown in Figure 2, parameter ($R_{F,e} - R_{F,s}$) is the flap length and $0.5(R_{F,e} + R_{F,s})$, the radial location of the centre of the flap, represents the flap location. Here, the length of the flap is limited to 5 % of the rotor radius to restrict the added mass and cost. Since the inner parts of the blade are aerodynamically less effective and since the flap cannot be installed at the tip of the blade, the position of the flap is limited between 60 % and 95 % of the rotor radius. The optimization problem of (3) is reformulated as follows:

$$\max P_{av} = f(X) \quad (4.a)$$

where

$$X = \{\beta_0(r), R_{F,s}, R_{F,e}\} \quad (4.b)$$

subject to:

$$P \le P_{rated} \quad (4.c)$$

$$M_{flap,opt} \le M_{flap,original} \quad (4.d)$$

$$R_{F,s} \ge 0.6R \quad (4.e)$$

$$R_{F,e} \le 0.95R \quad (4.f)$$

$$R_{F,e} - R_{F,s} \le 0.05R \quad (4.g)$$

The pretwist distribution $\beta_0(r)$ is defined using $n_{dp} = 5$ design points. The width of the flap d_F is considered as 10 % of the local chord c_F, where c_F is the chord @ $0.5(R_{F,e} + R_{F,s})$. The flap deployment angle is assumed to be limited to the lower and upper limits of 20 degrees: $\delta_{F,l} = -20°$ and $\delta_{F,u} = +20°$.

The optimum solution is found to have a pretwist distribution, as shown in Figure 4.a, with a flap extended between 70-75 % of the rotor radius. Figures 4.b through 4.d show the performances of original AWT-27 without installing flap, AWT-27 blades equipped with flap but with original pretwist, and AWT-27 blades equipped with flap with an optimized pretwist. It is evident that the addition of flap to the original blades without modifying them has some positive effect on the power capture capability (improving the average power from 43.9 kW to 44.8 kW and showing the increase of 2.1 %). However, this slight improvement comes at a cost of 4.6 % increase in the flap bending moment at the root (176.5 kNm versus 168.7 kNm). On the other hand, comparing the performances of the optimized blades equipped with flaps and the original blades, we observe a significant 8.84 % improvement in the average power (47.7 kW versus 43.9 kW) as well as a 2.9 % reduction in the root bending moment (163.8 kNm versus 168.7 kNm).

The behavior of the power curve of Figure 4.b for blades equipped with flap and optimized pretwist suggests that flap can be used instead of traditional pitch control system to regulate the rotor power at wind speeds above the rated speed. This is consistent with the behavior of blade root bending moment curve shown in Figure 4.d, in which the bending moment increases to its maximum value at a rated wind speed (similar to pitch-controlled rotors) and, then, decreases at higher wind speeds. A slight reduction in power curve at wind speeds above 23 m/s and increase in blade bending moment for wind speeds above 20 m/s result from flap saturation. A perfect power regulation and a continuous bending moment reduction at higher wind speeds (similar to pitch-controlled rotors) can be achieved by using a bigger flap or allowing higher deployment angles beyond $\pm 20°$.

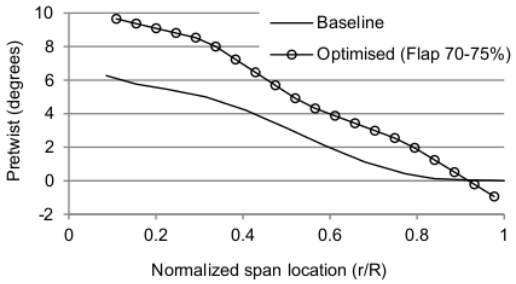

(a)

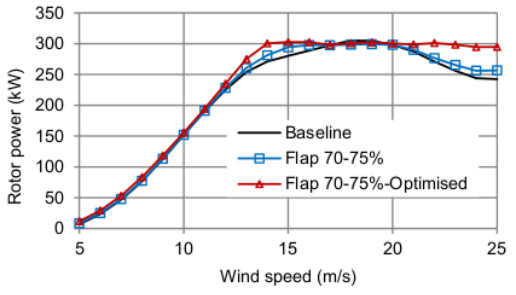

(b)

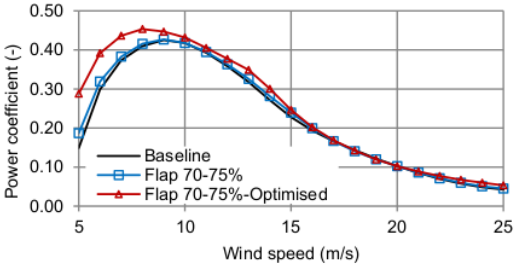

(c)

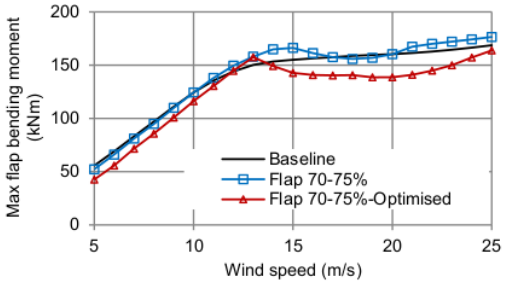

(d)

Figure 4. Blade with trailing edge flap @ 70-75 % of the span - Constant speed rotor

The optimization problem (4) can be also solved in the case of variable speed rotors, where all parameters are the same as those used in the case of constant speed rotor except the rotor speed which is treated here as a controlling parameter. For simulating the rotor speed, the following parameters are used: $\Omega_l = 30$ rpm, $\Omega_u = 65$ rpm, and $\varepsilon_\Omega = 0.1$ rpm. For the variable speed rotor, the optimum solution is found to have a pretwist distribution, as shown in Figure 5.a, with the optimum flap location between 70-75 % of the rotor radius. Figures 5.b to 5.d show the performance of the unit with original blades, original blades with flap, and optimized blade with flap.

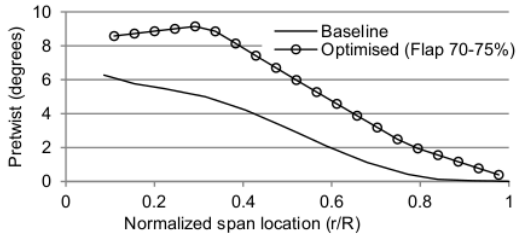

(a)

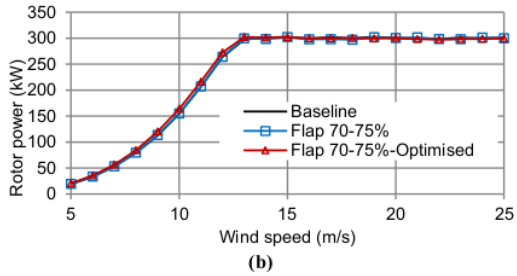

(b)

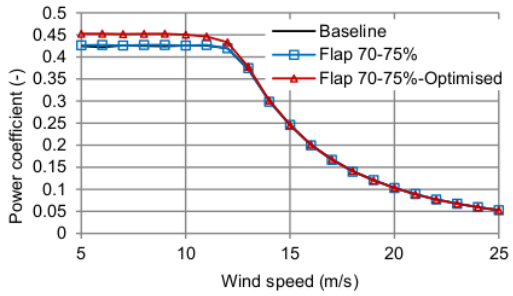

(c)

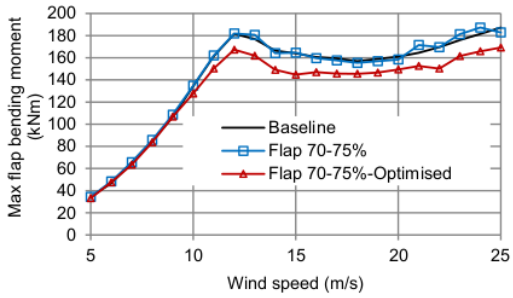

(d)

Figure 5. Blade with trailing edge flap @ 70-75% of the span – Variable-speed rotor

As expected, in the case of turbines with variable speeds, since the dominant controlling parameter is the rotor speed, the contribution of other active flow controllers, such as trailing edge flaps, in improving the energy capture capability is very small. This contribution, however, increases notably as a result of optimization (here, a 4.8 % increase in the average power from 49.7 kW to 52.1 kW). Moreover, with reference to Figure 5.d, one can see that the blade optimization leads to the reduction of blade loading as well (here, 9.6 % from 187.3 kNm to 169.2 kNm). Moreover, the same argument regarding flap saturation and its effect on the behavior of blade root bending moment curve can be made for rotors with variable speeds.

4.1. Parametric study

Reference [25] reports the results of a parametric study on exploring the potential benefit and effect of using trailing edge flaps on constant speed rotors. Here, by adopting the same approach, the effect of the size and location of flap on the power capture capability of variable speed rotors is investigated for 11 cases of different flap sizes and locations, as shown in Table 1. For each case, the optimum pretwist is found upon solving an optimization problem similar to that of (5.a), in which $X = \{\beta_0(r)\}$ with Constraint (5.c) as the only constraint applied. The results of performance simulation are shown in Figures 6 and 7.

In Figure 7.a, all flaps start at 60 % of the rotor radius (Cases 1 and 8 through 11 in Table 1). In Figure 7.b, all flaps have a span of 5 % of rotor radius (Cases 1 through 7 in Table 1). By using the data shown in Figure 7, the share of blade pretwist optimization in the power enhancement is shown in Figure 8.

Table 1. Studied flap lengths and flap locations (in % of R)

Case	$R_{F,s}$	$R_{F,e}$	Flap location $0.5(R_{F,e}+R_{F,s})$	Flap length $R_{F,e}-R_{F,s}$
1	60	65	62.5	5
2	65	70	67.5	5
3	70	75	72.5	5
4	75	80	77.5	5
5	80	85	82.5	5
6	85	90	87.5	5
7	90	95	92.5	5
8	60	70	65.0	10
9	60	75	67.5	15
10	60	80	70.0	20
11	60	85	72.5	25

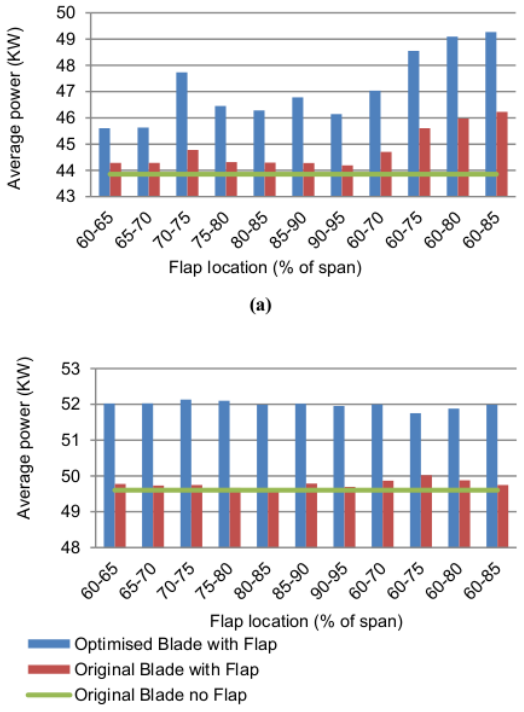

(a)

(b)

Figure 6. Average power for different flap sizes and locations: (a) constant speed [25] and (b) variable-speed rotors

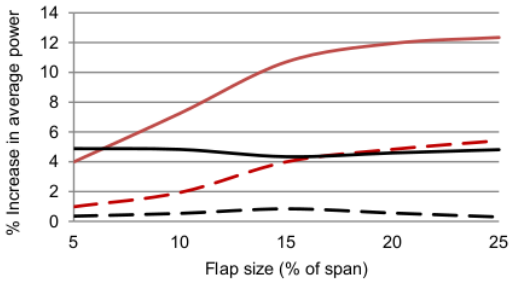

(a)

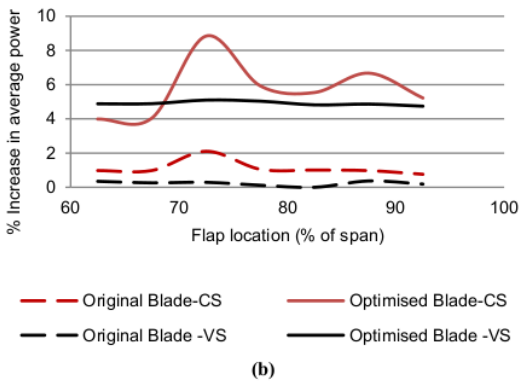

(b)

Figure 7. Effects of the (a) flap size and (b) flap location on the improvement in the average power

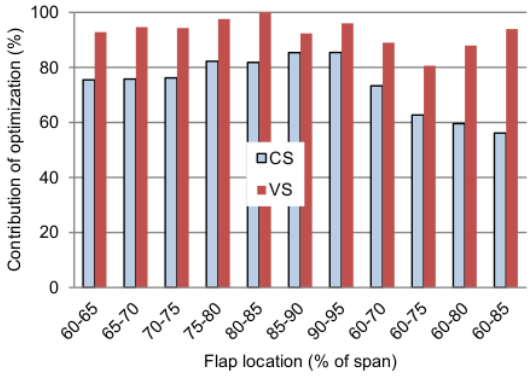

Figure 8. Contribution of optimization to the power enhancement

In view of these results, the following conclusions can be drawn:

- For CS rotors, the size of the flap has a significant effect on the amount of enhancement in the average power. This effect, however, reduces dramatically as the size increases (also reported in [25]).
- For CS rotors, the location of flap is a key parameter influencing the amount of improvement in the power extraction. The best location for placing a flap is at about 70 % of the blade span from the root of the blade (also reported in [25]).
- In contrast to CS rotors, neither the location of the flap nor its size affect the performance significantly. This is mainly due to having a rotor speed as the dominant controlling system in place.
- Effect of flap on CS is greater than that of flap on VS.
- Contribution of the pretwist optimization to enhancing the power capture capability in both CS and VS rotors is significant. Contribution of the blade optimization in VS rotors is greater than that in CS rotors.

Optimization has the highest effect on shorter flaps located towards the tip of the blade. This is due to the facts that the outer parts of the blade are aerodynamically more sensitive and that flow kinematics can be more optimized locally around shorter flaps.

5. POTENTIALS OF MICROTABS IN POWER ENHANCEMENT AND REGULATION

Since we are using a string of microtabs over a portion of the blade rather than a single microtab, the length of the string does not make a meaningful design variable. The reason is that some part of the string (the inner parts) might be always in a neutral position with no effect on the power. Therefore, we assume that the string of microtabs has a fixed length of 20 % of the span, extended from $R_{MT,s} = 0.7R$ to $R_{MT,e} = 0.9R$. The optimization problem of (4) is then reformulated as follows:

$$\max P_{av} = f(X) \quad (5.a)$$

where

$$X = \{\beta_0(r)\} \quad (5.b)$$

subject to:

$$P \le P_{rated} \quad (5.c)$$

$$M_{flap,opt} \le M_{flap,original} \quad (5.d)$$

Using $d^*_{MT} = 80$ % and $d^*_{MT} = 95$ % of the chord from the leading edge on the upper and lower surfaces, respectively, with an actuation height of $h^*_{MT} = 3.3$ % of the chord length, the blade is optimized for pretwist, as shown in Figure 9.a.

In Figures 9.b and 9.c, the curves representing the baseline blade and the baseline blade with microtabs are almost identical. With reference to Figure 9, it is evident that the baseline blades extract more or less the same amount of power, with or without microtab, unless the pretwist is optimized. The pretwist optimization leads to some improvement of 4.2 % in the average power (45.7 kW versus 43.9 kW).

By repeating the optimization problem above for the case of variable speed rotor, no improvement was observed due to the dominance of the rotor speed as the controlling parameter.

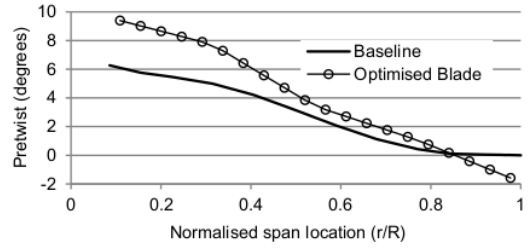

(a)

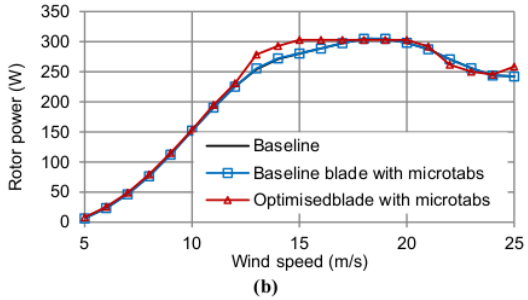

(b)

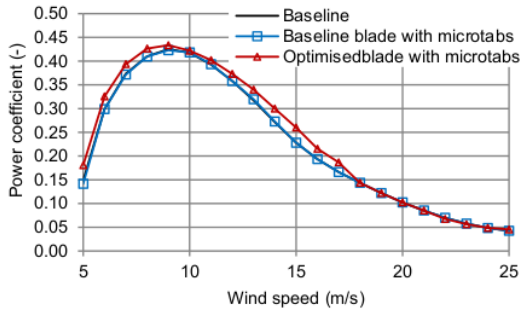

(c)

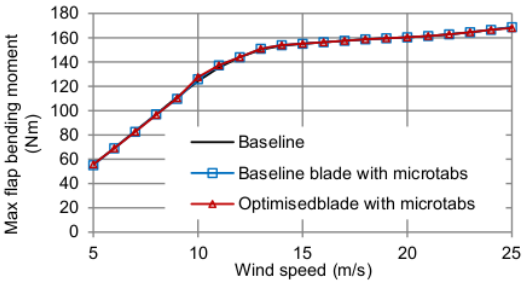

(d)

Figure 9. Microtab on optimised blades

6. SUMMARY AND CONCLUSION

Active flow controllers such as trailing edge flaps and microtabs were proposed and developed for damping 1P-3P cyclic and stochastic loads on wind turbine blades. Their effectiveness in load alleviation and their potential in increasing the lifespan of blades were proven through a series of researches during the past decade. This paper explored the effectiveness of these devices in power enhancement at low winds and power regulation at high winds towards answering the issue of whether these devices can be used with the dual function of load and power control.

The constant-speed stall-regulated 300 kW AWT 27 wind turbine was adopted as the case for studying the effect of trailing edge flaps and microtabs on power enhancement at low winds and power regulation at high winds. In all cases, the pretwist of the blades was optimized to ensure that the full potential of active flow controllers is realized without increasing the cost and mass of the blade (except for the added cost or mass of the active flow controller itself). The optimization objective was taken as the annual average power (to be maximised) with constraints on power (for power regulation) and flap bending moment of the blades at root (to ensure that the mass of the optimized blade is not larger than the mass of the original blade). The following conclusions can be drawn from the results of these case studies:

- In both constant speed and variable speed rotors, adding flaps to the original blades without pretwist optimization has some positive effect on the power capture capability. However, this slight improvement comes at the cost of an increase in blade loading. Optimized blades equipped with flaps can increase the annual average power and reduce blade loading at the same time for both constant speed and variable speed rotors. The effect of power

enhancement is more visible on constant speed rotors, while load reduction is more significant for variable-speed rotors. In variable-speed rotors, since the dominant controlling parameter is the rotor speed, the effect of adding trailing edge flap on improving the energy capture capability is lower.

- For variable-speed generators, neither the position nor the size of flap affects the extracted power significantly. On the other hand, in the case of constant-speed generators, the position of flap along the blade span plays a key role in influencing the amount of improvement in the rotor power. At the examined positions, it was found that the best location for positioning a flap was at about 70 % of the blade span. The flap size is also found to have a significant effect on the average power enhancement. However, this effect is not linear and reduces significantly as the size of flap increases.
- Contribution of the pretwist optimization to enhancing the power capture capability in both constant-speed and variable-speed rotors is significant. Contribution of the blade optimization to variable-speed rotors is greater than that to constant speed rotors. Optimization has the highest effect on shorter flaps located towards the tip of the blade. This is due to the facts that the outer parts of the blade are aerodynamically more sensitive and that flow kinematics can be more optimized locally around shorter flaps.
- Flap is much more efficient than microtabs in power control. The baseline blades extract almost the same amount of power, with or without microtab. However, with an optimized pretwist, microtabs can improve the power produced by up to 4 %.

Most likely, more improvements could be made by removing some of the optimization constraints. For example, removing Constraint (5.g) $R_{F,e} - R_{F,s} \leq 0.05R$ allows the optimizer to explore the longer flaps. The addition of chord as a design variable in the optimization process needs conducting a cost analysis, but makes the design space more flexible and, therefore, provides a greater chance for finding superior solutions in terms of power enhancement and load reduction compared to the reported ones.

7. ACKNOWLEDGEMENT

This research has received no external funding.

NOMENCLATURE

AF	Aerofoil index
c	Chord length (m)
c_F	Chord length at flap location (m)
c_M	Chord length at microtab location (m)
C_D	Drag coefficient
C_L	Lift coefficient
C_M	Pitching moment coefficient
d_F	Flap width (m)
d_{MT}	Microtab distance from the leading edge (m)
h_{MT}	Microtab actuation height (m)
M_{flap}	Blade flapwise bending moment at root (Nm)
m_{blade}	Blade mass (kg)
pitch	Pitch angle (°)
P	Rotor power (W)
P_{av}	Site average power (W)
P_{rated}	Rated power (W)
R	Rotor radius (m); probability density function
$R_{F,e}$	Flap outboard radial location (m)
$R_{F,s}$	Flap inboard radial location (m)
$R_{MT,e}$	Microtab outboard radial location (m)
$R_{MT,s}$	Microtab inboard radial location (m)
r	Span location (m)
s_{MT}	Single microtab length (m)
t_{max}	Aerofoil maximum thickness (% of chord)
V	Wind speed at hub height (m/s)
V_i	Cut in wind speed (m/s)
V_o	Cut out wind speed (m/s)
V_{rated}	Rated wind speed (m/s)
Greek letters	
α	Angle of attack
β_0	Blade pretwist (°)
β_e	Blade elastic twist (°)
δ_F	Flap deployment angle (°)
φ	Inflow angle (°)
Ω	Rotor speed (rpm)
Subscripts	
F	Flap
l	Lower limit
MT	Microtab
opt	Optimum
origin	Original
u	Upper limit
Superscript	
*	Normalised

REFERENCES

1. Barlas, T.K. and van Kuik, G.A.M., "Review of state of the art in smart rotor control research for wind turbines", ***Progress in Aerospace Sciences***, Vol. 46, No. 1, (2010), 1-27. (https://doi.org/10.1016/j.paerosci.2009.08.002).
2. Yuan, Y. and Tang, J., "On advanced control methods toward power capture and load mitigation in wind turbines", ***Engineering***, Vol. 3, No. 4, (2017), 494-503. (https://doi.org/10.1016/J.ENG.2017.04.023).
3. Menezes, E.J.N., Araújo, A.M. and da Silva, N.S.B., "A review on wind turbine control and its associated methods", ***Journal of Cleaner Production***, Vol. 174, (2018), 945-953. (https://doi.org/10.1016/j.jclepro.2017.10.297).
4. Larsen, T.J., Madsen, H.A. and Thomsen, K., "Active load reduction using individual pitch, based on local blade flow measurements", ***Wind Energy***, Vol. 8, No. 1, (2005), 67-80. (https://doi.org/10.1002/we.141).
5. van Engelen, T.G., "Design model and load reduction assessment for multirotational mode individual pitch control (higher harmonics control)", ***Proceedings of European Wind Energy Conference***, Athens, (2006). (https://publicaties.ecn.nl/PdfFetch.aspx?nr=ECN-RX--06-068).
6. Johnson S.J., Baker J.P., van Dam, C.P. and Berg, D., "An overview of active load control techniques for wind turbines with an emphasis on microtabs", ***Wind Energy***, Vol. 13, No. (2-3), (2010), 239-253. (https://doi.org/10.1002/we.356).
7. Bæk, P., Gaunaa, M., Sørensen, N.N. and Fuglsang, P., "Comparative study of distributed active load control concepts for wind turbine blades", ***Proceedings of Science of Making Torque from Wind Conference***, Heraklion, Greece, (2010), 611-617. (https://doi.org/10.2514/6.2011-348).
8. Macquart, T., Maheri, A. and Busawon, K., "Microtab dynamic modelling for wind turbine blade load rejection", ***Renewable Energy***, Vol. 64, (2014), 144-152. (https://doi.org/10.1016/j.renene.2013.11.011).
9. Macquart, T. and Maheri, A., "Integrated aeroelastic and control analysis of wind turbine blades equipped with microtabs", ***Renewable Energy***, Vol 75, (2015), 102-114. (https://doi.org/10.1016/j.renene.2014.09.032).
10. Macquart, T., Maheri, A. and Busawon, K., "A decoupling control strategy for wind turbine blades equipped with active flow controllers", ***Wind Energy***, Vol. 20, (2017), 569-584. (https://doi.org/10.1002/we.2024).
11. Chen, H. and Qin, N., "Trailing-edge flow control for wind turbine performance and load control", ***Renewable Energy***, Vol. 105, (2017), 419-435. (https://doi.org/10.1016/j.renene.2016.12.073).

12. Oltmann, N.C., Sobotta, D. and Hoffmann, A., "Load reduction of wind turbines using trailing edge flaps", ***Energy Procedia***, Vol. 136, (2017), 176-181. (https://doi.org/10.1016/j.egypro.2017.10.316).
13. Zhuang, C., Yang, G., Zhu, Y. and Hu, D., "Effect of morphed trailing-edge flap on aerodynamic load control for a wind turbine blade section", ***Renewable Energy***, Vol. 148, (2020), 964-974. (https://doi.org/10.1016/j.renene.2019.10.082).
14. Chen, Z.J., Stol, K.A. and Mace, B.R., "Wind turbine blade optimisation with individual pitch and trailing edge flap control", ***Renewable Energy***, Vol. 103, (2017), 750-765. (https://doi.org/10.1016/j.renene.2016.11.009).
15. Ebrahimi, A. and Movahhedi, M., "Wind turbine power improvement utilizing passive flow control with microtab", ***Energy***, Vol. 150, (2018), 575-582. (https://doi.org/10.1016/j.energy.2018.02.144).
16. Maheri, A., "Simulation of wind turbines utilising smart blades", ***Journal of Thermal Engineering***, Vol. 2, No. 1, (2016), 557-565. (https://doi.org/10.18186/jte.01522).
17. Maheri, A., "Multiobjective optimisation and integrated design of wind turbine blades using WTBM-ANSYS for high fidelity structural analysis", ***Renewable Energy***, Vol. 145, (2020), 814-834. (https://doi.org/10.1016/j.renene.2019.06.013).
18. Maheri, A., Noroozi, S., Toomer C. and Vinney, J., "WTAB, a computer program for predicting the performance of horizontal axis wind turbines with adaptive blades", ***Renewable Energy***, Vol. 31, No. 11, (2006), 1673-1685. (https://doi.org/10.1016/j.renene.2005.09.023).
19. Maheri, A., Noroozi, S., Toomer C. and Vinney, J., "Damping the fluctuating behaviour and improving the convergence rate of the axial induction factor in the BEMT-based rotor aerodynamic codes", ***Proceedings of European Wind Energy Conference and Exhibition 2006, EWEC (2006)***, Athens, Greece, Vol. 2, (2006), 1176-1179. (https://www.researchgate.net/publication/277016534_Damping_the_fluctuating_behaviour_and_improving_the_convergence_rate_of_the_axial_induction_factor_in_the_BEMT_based_rotor_aerodynamic_codes).
20. Macquart, T., Maheri, A. and Busawon, K., "Improvement of the accuracy of the blade element momentum theory method in wind turbine aerodynamics analysis", ***Proceedings of 2nd International Symposium on Environment Friendly Energies and Applications***, Newcastle, UK, (2012). (https://doi.org/10.1109/EFEA.2012.6294047).
21. Drela, M., "XFOIL: An analysis and design system for low Reynolds number airfoils", Low Reynolds number aerodynamics, Lecture notes in engineering, Mueller, T.J. (eds.), Springer, Berlin, Heidelberg, (1989). (https://web.mit.edu/drela/Public/papers/xfoil_sv.pdf).
22. Maheri, A., Macquart, T., Safari, D. and Maheri, M., "Phenotype building blocks and geometric crossover in structural optimisation", ***Proceedings of ECT2012: Eighth International Conference on Engineering Computational Technology***, Dubrovnik, Croatia, (2012). (https://doi.org/10.4203/ccp.100.51).
23. Kahwash, F. and Maheri, A., "A genetic algorithm for optimal distribution of aerofoils on wind turbine blades", ***Proceedings of 1st International Conference on Engineering of Tarumanagara (ICET 2013)***, Jakarta, (2013). (https://www.researchgate.net/publication/261285892).
24. Poore, R., "NWTC AWT-26 research and retrofit project -Summary of AWT-26/27 turbine research and development", NREL report NREL/SR-500-26926, (2000). (https://www.nrel.gov/docs/fy00osti/26926.pdf).
25. Wiratama, I.K. and Maheri, A., "Optimal design of wind turbine blades equipped with flaps", ***ARPN Journal of Engineering and Applied Sciences***, Vol. 9, No. 9, (2014), 1511-1515. (http://www.scopus.com/inward/record.url?eid=2-s2.0-84907258786&partnerID=MN8TOARS).

12.Performance of Microtabs and Trailing Edge Flap

ORIGINALITY REPORT

4%	3%	2%	4%
SIMILARITY INDEX	INTERNET SOURCES	PUBLICATIONS	STUDENT PAPERS

PRIMARY SOURCES

1	docplayer.net Internet Source	2%
2	Submitted to University of Aberdeen Student Paper	2%

Exclude quotes	Off	Exclude matches	< 2%
Exclude bibliography	Off		

12.Performance of Microtabs and Trailing Edge Flap

GRADEMARK REPORT

FINAL GRADE

/0

GENERAL COMMENTS

Instructor

PAGE 1

PAGE 2

PAGE 3

PAGE 4

PAGE 5

PAGE 6

PAGE 7

PAGE 8

PAGE 9